

Research Article

Chemistry

Fabrication, Properties, and Stability of Frankincense Oil and Fatty Chitosan/Polyvinyl Alcohol-Based Wound-Healing Hydrogels

Tamer M. Tamer¹, Samia El-Sigeny², Sarah Shoman², Hanaa Mansour^{2*}

¹Polymer Materials Research Department, Advanced Technology and New Materials Research Institute (ATNMRI), City of Scientific Research and Technological Applications (SRTA-City), Alexandria, 21934, Egypt

²Department of Chemistry, Faculty of Science, Kafrelsheikh University, Kafrelsheikh, 33516, Egypt

*Corresponding author: Hanaa Mansour

E-mail: hanaa.mansour@sci.kfs.edu.eg

Received: 11/1/2024

Accepted: 8/2/2024

KEY WORDS

Frankincense extract, Hydrogel, N-Hexadecanyl chitosan, polyvinyl alcohol, Wound therapy

ABSTRACT

As a hydrogel, the wound dressings made of polymers and Frankness Oil (Frank) can work incredibly well. The goal of the current study is to prepare Frank sponge hydrogels with fatty N-hexadecanyl chitosan derivatives as an antibacterial agent into polyvinyl alcohol (PVA). The bioactivity and physicochemical performance of PVA/Frank-based polymeric hydrogels were assessed. The polymeric interactions, surface morphology, water absorption capability, thermal stability, thrombogenicity and hemocompatibility were investigated by FT-IR, SEM, swelling ratio, and DSC. SEM photographs show that the PVA sponge hydrogel has a characteristic porosity structure and a noticeably lamellar appears and DSC demonstrates the thermal stability of the hydrogels. Furthermore, they demonstrated fast bleeding control because of their high-water absorption, with the PVA/Frank hydrogel having the highest water uptake efficiency (383.5%). The findings also demonstrate that Frank oil significantly impacts the degradation rate, with the PVA/Frank/DNHD-CS hydrogel exhibiting the greatest weight loss of up to 35%. The antibacterial activity was examined, and the antioxidants were tested using the DPPH assay. According to the results, PVA/Frank/CS had the strongest antibacterial activity against *B. cereus* (80%). Using Frank oil in sponges with PVA/Frank hydrogel resulted in a considerable increase in ABTS⁺ radical scavenging activity, reaching 46% (g GAE/g film). All sponge hydrogels had hemolysis rates of less than 2%, indicating good blood compatibility and suitability for intravenous injection.

These findings suggest that the hydrogels containing Frank have potential use as an antibacterial and antioxidant agent for wound care, as well as for developing novel biomaterials for dressings.

Introduction

Wound healing is a well-known physiological process that the skin goes through in response to injury and is distinguished by the interaction of numerous interconnected stages, including haemostasis, inflammation, cellular proliferation, and tissue remodeling (Berthet *et al.*, 2017; Tamer *et al.*, 2018). The body starts vascular contraction and blood coagulation procedures after a skin wound, which stops continuous bleeding and prevent the invasion of dangerous germs. Additionally, blood clots act as a framework that supports dermal cell migration to the site of injury, promoting wound healing and subsequent tissue remodeling (Pereira *et al.*, 2016; Gurtner *et al.*, 2008). However, over an extended period, hemorrhaging has repeatedly emerged as the major cause of fatality among both non-combatants and military people. Trauma victims are more likely to die during the first hour of an event (King, 2019; Alarhayem *et al.*, 2016), highlighting the critical importance of quick hemorrhage control using blood clotting-promoting therapies. Uncontrolled bleeding can have serious consequences, including site inflammation and susceptibility to microbial infections (Ma *et al.*, 2020), both of which slow down the healing process. Membranes, electro-spun nanofibers, and hydrogel are

wide used as wound dressings, each with their own unique compositions (Guo *et al.*, 2021; Wang *et al.*, 2017). Hydrogel-based wound dressings, however, provide a few unique benefits over other types of dressings, such as the ability to absorb excessive wound exudates, create a cool environment on the wound surface to reduce discomfort, and maintain the optimal moisture level in the wound bed. These features facilitate the migration and multiplication of dermal cells (Wang *et al.*, 2019; Zhao *et al.*, 2020). Hydrogels are also frequently used as hemostatic dressings in cases of severe bleeding because of the noteworthy adhesive qualities they display (Peng *et al.*, 2021; Zhao *et al.*, 2018; Ren *et al.*, 2020). Injuries with non-compressible visceral bleeding and wounds with uneven geometries can be efficiently filled and sealed with hydrogels. Under normal coagulation conditions, adhesive hydrogels function effectively compared to conventional hemostatic materials that contain fibrin (Chan *et al.*, 2015; Baylis *et al.*, 2015). These hydrogels interact with the surrounding tissue to quickly create a blockage that stops future bleeding, principally relying on the presence of thrombin and fibrinogen in the blood (Kim *et al.*, 2021). Although injectable hydrogels have the ability to

operate as hemostatic agents (**Zhao et al., 2018**), their application is constrained by the poor mechanical qualities of these materials. The suffering associated with the replacement or removal of injectable hydrogels is the potential downside for patients, especially those who have sustained major wounds (**Sultana et al., 2021**). Because of their unique architecture, which provide them a certain level of mechanical stability, 3D sponges with antibacterial, hemostatic, and antioxidant capabilities are therefore useful. Furthermore, it is essential to stress that structural dimensionality plays a critical function in aiding the adhesion and proliferation of cells that are recruited to aid in the process of wound healing (**Shefe et al., 2017**). Various formulations for sponge hydrogel wound dressings with antibacterial and antioxidant properties have been developed which augmented with either natural extracts or antibacterial and anti-inflammatory drugs (**Haidari et al., 2020; Haidari, et al., 2021**). They showed how effective they were at slowing down the growth of several dangerous bacteria and accelerating the healing of infected wounds. Cheng *et al* have prepared a wound dressing with potent hemostatic and antimicrobial characteristics by developing a hydrogel based tannic acid and polyvinyl alcohol (PVA) (**Cheng et al., 2022**). Recent studies have shown that PVA and chitosan

hydrogels are excellent at accelerating the healing of damaged skin due to their antibacterial, antioxidant, and hemostatic qualities, as well as their adhesive and self-healing properties (**He et al., 2022; Guo et al., 2022**). Other studies showed that multifunctional hydrogel wound dressings, made of carboxymethyl chitosan and oxidized dextran/sodium alginate, are essential for promoting wound closure in wounds contaminated with dangerous bacteria (**Zhou et al., 2022; Xie et al., 2022**).

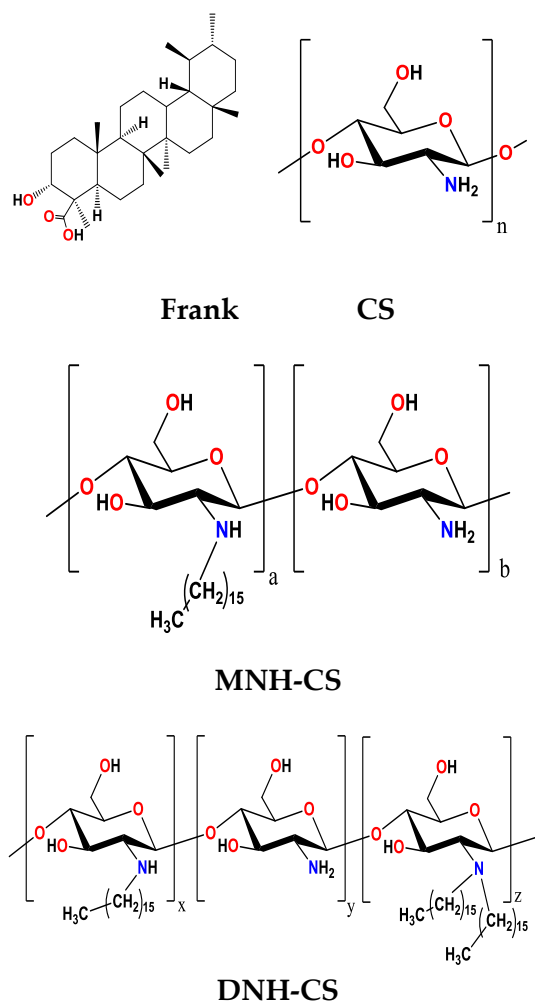
According to earlier investigations (**Fang et al., 2019**), porous sponges with extraordinary mechanical properties and exceptional biocompatibility were prepared using PVA as the basis material. Physical cross-linking techniques may be used in the manufacture of PVA sponges to reduce the potential negative consequences of using hazardous chemical cross-linking agents in critical applications. In this case, a sequential freeze-thaw process can be used to cross-link PVA-based sponges, with the crystalline clusters serving as the network nodes (**Qi et al., 2015; Chen et al., 2016**). The second most prevalent polymer after cellulose, chitosan (CS), a naturally occurring polymer has numerous biological features, including antibacterial activities (**Kenawy et al., 2019; Omar et al., 2019**), anticancer activity (**Tian et al., 2021; Shaban et al., 2019**), antioxidant

properties (Abdelrazik *et al.*, 2016), hemostatic activity (Lestari *et al.*, 2020), drug carriers (Mohy Eldin *et al.*, 2015), and wound healing (Tamer *et al.*, 2020; Hassan *et al.*, 2021; Raafat *et al.*, 2009; Li *et al.*, 2016). Therefore, the use of chemical modifications to CS's functional groups holds enormous promise for the preparation of novel materials with enhanced properties (Le-Vinh *et al.*, 2019).

Frankincense (Frank), which refers to the exudates made from the periderm of arboreal specimens associated with the *Boswellia* taxonomic classification, is an example of a product obtained from a botanical (Hamedpur *et al.*, 2013; Sharma *et al.*, 2009). As a natural alternative to conventional medicine, Frank has been used to treat a variety of ailments, including cancer, arthritis, asthma, chronic pain syndrome, and cognitive impairments (Bekana *et al.*, 2014) and also has calming analgesic and antibacterial properties (Khalifa *et al.*, 2023; Bakhit *et al.*, 2021; Yagi *et al.*, 2016). Additionally, earlier research has shown that Frank resin extract is excellent at reducing skin irritability and redness while also promoting consistent skin pigmentation. By using this material, the texture of the skin may be improved and a variety of skin problems, such as wrinkles, skin infections, irritation, wounds, dry lips, acne, scars, and cold sores can be treated

(Saied *et al.*, 2020; Han *et al.*, 2017; Zhu *et al.*, 2017; Guan *et al.*, 2017; Cao *et al.*, 2019).

In the present study, CS, mono-N-hexadecanyl (MNHD-CS) and di-N-hexadecanyl chitosan derivatives (DNHD-CS) (Mansour *et al.*, 2022) (Scheme 1) are used in a synergistic manner with Frank with the goal is to increase the hydrogels' biological effectiveness and to use as wound healing materials with hemostatic, antibacterial, and antioxidant properties.



Scheme (1): Structure representation of Frank, CS, MNH-CS, and DNH-CS.

By using a freezing and thawing procedure on PVA and taking inspiration from CS, MNHD-CS and DNHD-CS as well as Frank, novel cross linked three-dimensional network sponges were prepared. To assess their potential as effective wound dressings, sponges' physicochemical and biological properties were also evaluated.

Materials and methods

Materials and Bacterial Strains

PVA (Mw = 72 kDa) and CS (MW. 100,000–300,000 Dalton) were obtained from Across Organics (New Jersey, USA). MNHD-CS and DNHD-CS derivatives have been prepared in our laboratory as reported previously (**Mansour et al., 2022**). Frank, sodium hydroxide, dimethyl sulfoxide (DMSO), and acid citrate dextrose solution (ACD), folin–ciocalteu, gallic acid, 2,2-diphenyl-1-picrylhydrazyl (DPPH), and 2,20-azino-bis(3-ethylbenzothiazoline-6-sulphonic acid (ABTS) were acquired from Sigma-Aldrich Co., Ltd. in St. Louis, Missouri, United States. Gibco was acquired by Dulbecco's Modified Eagle Medium (DMEM) and trypsin (ThermoFisher Scientific, Waltham, MA, USA). Bioshop supplied yeast extract, tryptone, and sodium chloride (Canada Inc., Ontario, CA, Canada). Gram-positive and Gram-negative bacteria, *Escherichia coli* (*E. coli*), *Pseudomonas aeruginosa* (*P. aeruginosa*), *Staphylococcus aureus* (*S.*

aureus), and *Bacillus cereus* (*B. cereus*), were used to test the antibacterial abilities of the produced dressings. The bacterial strains were inoculated into LB medium with 10 g/L NaCl, 10 g/L peptone, and 5 g/L yeast extract prior to the antibacterial experiment, and they were then incubated at 37°C at 150 rpm for 18 hours.

Methodology

Preparation of Sponges

A freezing-thawing cycle methodology was used to produce the PVA sponge composites in accordance with reported procedures with slight modification (**Tamer et al., 2021; Tamer et al., 2022**). Briefly; 20 ml of 5% (w/v) PVA, 0.5 ml of Frank, and 0.3 g/5 ml of CS and CS derivatives were thoroughly mixed before being subjected to sonication and stirred for an hour. The mixture was then put into Petri plates and put through five cycles of -20 °C freezing for 18 hours and -25 °C thawing for 6 hours. Along with a PVA control sponge, samples of sponges with varied amounts of Frank and CS derivatives were identified as PVA, PVA/Frank, PVA/CS, PVA/Frank/CS, PVA/MNHD-CS, PVA/Frank/MNHD-CS, PVA/DNHD-CS, and PVA/Frank/DNHD-CS, respectively. The produced sponges were lyophilized after being flash-frozen in liquid nitrogen for ten minutes.

Characterization of the Sponges

FT-IR (KBr) apparatus (Shimadzu 8400S, Kyoto, Japan) was set up to do a total of forty scans on each sponge between the wavelengths of 400 and 4000 cm^{-1} . Each sample was coated with a thin layer of gold under vacuum before being examined using SEM (Joel Jsm 6360LA, Tokyo, Japan) to look at the morphological alterations of the produced sponges. Thermal gravimetric analyzer (TGA) (Shimadzu 50/50H, Kyoto, Japan) with a heating rate of 10 $^{\circ}\text{C}/\text{min}$ and a nitrogen flow of 30 mL/min was used to measure 5 mg of each film in the temperature range of 20-600 $^{\circ}\text{C}$. Sponge dried for 24 hours at 50 $^{\circ}\text{C}$ in a vacuum oven before being weighed to determine the gel fraction. After that, the sponges were re-swollen in distilled water for 24 hours until the equilibrium swelling threshold for eliminating soluble PVA was attained. The sponges were then weighed and dried in a vacuum oven at 50 $^{\circ}\text{C}$. Each experiment was conducted five times, and the gel fractions were calculated using the following Equation:

$$\text{Gel fraction (\%)} = \frac{W_e}{W_i} \times 100 \quad (1)$$

Where W_e and W_i refer to the weights of the dried sponge and swollen sponge, respectively. The sponges' capacity to swell was determined by weighing them after being immersed in water for a while.

500 ml of distilled water were added after 1 g of dry sponge was dipped into them. Dynamic Swelling was done at 25 $^{\circ}\text{C}$ until equilibrium was reached. Each swelled sample was removed at regular intervals and weighed after any water that had gathered on the surface had been carefully wiped away with filter sheets. The swelling ratios were calculated using the following equation five times for each experiment:

$$\text{Swelling ratio (\%)} = \frac{W_s - W_d}{W_d} \times 100 \quad (2)$$

Where W_s denotes the weight of the swollen sponge, while W_d refers to the weight of the sponge at the initial time. The measurements were performed in accordance with the procedure outlined by Yin et al to estimate the porosity of the sponges (Yin *et al.*, 2007). The dried weights of the sponges were calculated following a two-hour drying process at 50 $^{\circ}\text{C}$ in a vacuum oven. The samples were then submerged in 100% ethanol for four hours. The expanded sponges were wiped with filter paper to remove extra ethanol before being weighed. Following that, five times through the porosity analyses, Equation was used to determine porosity:

$$\text{Porosity (\%)} = \frac{W_2 - W_1}{\rho V} \times 100 \quad (3)$$

Where W_1 and W_2 represent the weight of the sponge before and after immersion in

absolute ethanol, V represents the volume of the sponge, and ρ represents the density of absolute ethanol. Dry sponges were weighed, dipped in 3 mL PBS (0.1 M, pH 7.4), kept at 37 °C, and removed at intervals to be gently cleaned with soft papers to remove excess water from their surfaces. The samples were then gently dried under vacuum conditions before being weighed. All experiments were carried out with five independent replications.

Antibacterial Assay

The antibacterial assessment of the sponges was determined by measuring optical densities and colony-forming units (CFU) per ml. First, overnight bacteria strains cultures were diluted in LB medium before and their turbidities were adapted in accordance with the McFarland 0.5 standard at 625 nm with 2×10^8 CFU/ml (Hasan *et al.*, 2019; Hassan *et al.*, 2022). Next, 100 mL of the diluted bacterial cultures were then added to 10 mL LB medium containing 50 mg of tested sponges, followed by 18 hours of incubation at 37°C with shaking conditions at 150 rpm. As a comparison, bacterial cultures without sponges were used as controls. After incubation, the antibacterial ability was tested by measuring of bacterial growth inhibition using a spectrophotometer at 600 nm, and then the ratio of bacterial growth

inhibition was calculated using Equation (4):

$$\text{Bacterial growth inhibition (\%)} = \frac{OD_c - OD_i}{OD_c} \times 100 \quad (4)$$

Where OD_c and OD_i are the optical densities of untreated and treated bacterial cultures, respectively.

Bioactive evaluation of the Sponges Phenolic contents determination

Phenolic contents of the sponges were determined by reducing the yellow Folin-Ciocalteu reagent to a blue compound. First, 50 mg of each membrane was immersed in 5 ml of ethanol in order to extract the frank oil content. 0.5 mL of sponge supernatant was then added to 2.0 ml of Folin–Ciocalteu reagent (10%, v/v), followed by the addition of 2 ml of sodium carbonate solution (7.5%, w/v). The mixture was kept at 50 °C for 5 minutes, after which the absorbance was measured at 760 nm using a spectrophotometer. The measurements were repeated five times and compared to the stranded curve for gallic acid (0–100 g) solutions.

Antioxidant activity evaluation

ABTS assay was carried out for this study through generation of radical cations by the reaction of an aqueous $K_2S_2O_8$ (3.30 mg) in 5 ml water solution with 17.2 mg ABTS. The resulting bluish-green radical cation solution was then stored overnight below 0 degrees Celsius and in the dark. Afterward, 1 ml of the

solution was diluted to a final volume of 60 mL with deionized water and labelled as the ABTS^{•+} solution. For the measurement of total phenolic content, the samples were extracted as described above. Then, 0.1 mL of leachate from each sponge was added to 2.0 ml of ABTS^{•+} solution. The ABTS^{•+} examination was conducted five times, and the absorbance at 730 nm was evaluated at several time periods.

Hemolysis experiments

Hemolysis evaluation of the sponges was carried out with a few minor modifications as previously reported by Yuan (Yuan *et al.*, 2024). To do this assessment, anticoagulated blood 9 ml of blood was mixed with 1 ml of anticoagulant acid citrate dextrose solution (ACD). About 1 cm² of each film was submerged in phosphate buffer solution (PBS, pH 7.0) for 72 hours at 37 °C prior to the tested membranes being exposed to blood. The sponges were then submerged in 1 ml of ACD blood for three hours at 37 °C after the PBS had been removed. Comparable amounts of ACD blood were mixed with 7 ml of PBS and water to get the negative and positive control tubes. For proper blood-film contact, the tubes were carefully inverted three times every 30 minutes. The liquids were then transferred to new tubes and centrifuged for 15 minutes at 200 rpm to remove any remaining material. The

wavelength of the haemoglobin produced during hemolysis was determined using a spectrophotometer (Model Ultrospec 2000). Five duplicates of each measurement were used throughout, and Equation 5 was used to calculate the hemolysis ratio.

$$\text{Hemolysis (\%)} = \frac{OD_m - OD_n}{OD_p - OD_n} \times 100 \quad (5)$$

Where OD_m represents the absorbance of a tested sponge, OD_n represents the absorbance of the negative control, and OD_p represents the absorbance of the positive control.

Thrombogenicity tests

Thrombogenicity experiments were done using a gravimetric method to estimate how much thrombus was present on the surface of the synthetic sponges. ACD blood was created as previously demonstrated. For 48 hours, membranes were submerged in PBS at 37 °C. Following the incubation period, the PBS was removed, and the ACD blood was applied over the components that had undergone inspection. A positive control was also created at the same time by introducing the same quantity of ACD blood to an empty Petri dish. To encourage the blood clotting response, 20 ml of a 10 M calcium chloride solution was sprayed onto the sponges. 5 ml of water was added to cease the reactions after 45 minutes. Following this, the clots were joined with an additional 5 ml of a

36% formaldehyde solution, dried, and weighed. Five further thrombogenicity tests were reported.

Result and discussion

Characterization and Functional Group Analysis

In the current study, novel crosslinked three-dimensional sponges were developed by freezing and thawing PVA and drawing inspiration from Frank, CS, MNHD-CS, and DNHD-CS. Fig. (1) showed FT-IR spectra of the composite sponge hydrogels. The predominant reason of the PVA sponge's hydrophilic characteristics is the presence of hydroxyl groups in the PVA chains, which are characterized by stretching vibration bands between 3200 and 3400 cm^{-1} (Mansur *et al.*, 2004; Mansur *et al.*, 2008). Furthermore, at 2922 cm^{-1} , methyl groups are appeared with both symmetrical and asymmetrical CH stretching vibrations. Characteristic bands at 2841 and 1643 cm^{-1} correspond to the vibration of the $-\text{CH}_2$ group and the acetyl carbonyl groups, respectively. Moreover, at 1444 cm^{-1} , the asymmetrical and symmetrical CH bending vibrations of the methyl group were seen. The band at around 1460 cm^{-1} corresponds to N–H bending vibration is present in the sponges containing CS and MNHD–CS. Peaks at 1315 and 1076 cm^{-1} are assigned to C–N and C–O–H groups stretching, respectively. In addition to the pre-

existing bands assigned in PVA sponges, the addition of Frank leads to the appearance of a separate peak around 1445 cm^{-1} . A broad band between 3650 cm^{-1} and 3100 cm^{-1} , associated with the stretch of the O–H bonds, was clearly observed. As shown in the gravimetric analysis, the hydrogels were hygroscopic and had a great tendency to absorb water. This signal includes both Frank and chitosan O–H structure and water in its different strengths due to the hydrogen bonds formed. Because most important Frank signals overlap with important bands in the hydrogels, it is difficult to appreciate significant changes, although variations in signal intensities indicate the presence of Frank in the hydrogels.

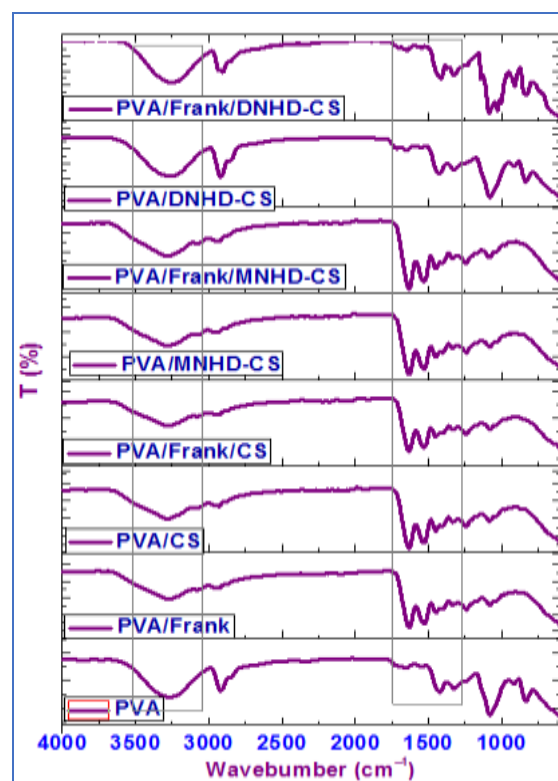


Fig. (1): FT-IR spectra of composite sponge hydrogels

Surface Morphology

To examine the microstructures of the prepared sponges, SEM technique was used (Fig. 2). Pure PVA sponges have a morphological surface with fewer pores but when combined with Frank, CS, MNHD-CS and DNHD-CS, the PVA hydrogel composites' three-dimensional structures were found to have asymmetrical patterns and rough connecting structures, as shown in (Fig. 2). Contrarily, in order to efficiently absorb excessive exudate and interact with blood, which facilitates the desired haemostatic outcome; haemostatic wound dressings must forge a strong link with the injuries (Zhou *et al.*, 2021; Fan *et al.*, 2020).

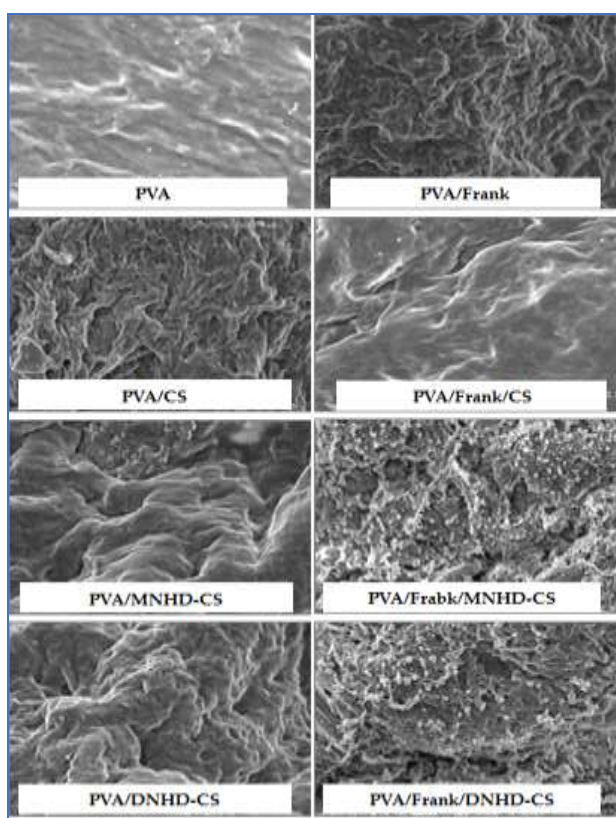


Fig. (2): SEM images reveal the surface morphologies of composite sponges.

Thermal Analysis

The examination of biomaterials' thermal characteristics is crucial for determining whether they are commercially viable for use in medicine (Liu *et al.*, 2019; Li *et al.*, 2014). TGA and DSC experiments were therefore used to examine the PVA composite hydrogel's thermal behavior. TGA results for the composite hydrogels are shown in Fig. (3). In all of the hydrogel samples, three different weight decreases were noticed. When the temperature of the composite sponge hydrogel was raised from room temperature to 200 °C, the weight of the hydrogel first decreased, dropping by 7.48% in comparison to the weight of the pure hydrogel made of PVA. This occurrence is caused by water trapped by hydrophilic hydroxyl groups inside the polymer matrix evaporating. The recorded percentages for the different combinations are 8.1%, 11.76%, 10.94%, 8.64%, 12.77%, 11.94%, and 9.14% for PVA/Frank, PVA/CS, PVA/Frank/CS, PVA/MNHD-CS, PVA/Frank/MNHD-CS, PVA/DNHD-CS, and PVA/Frank/DNHD-CS, respectively which show an upward trend. Within the temperature range of 220 to 350 °C, the hydrogels as a whole showed a following notable loss in weight, which may be due to the removal of hydroxyl groups and the emergence of polyene macromolecules. The presence of chitin or chitin derivatives at this stage

affects the weight loss because it takes place in the same area as the damaging breakdown of the CS pyranose ring. Table (1) simply presents the important data regarding the value and T_{50} of the stages of degradation.

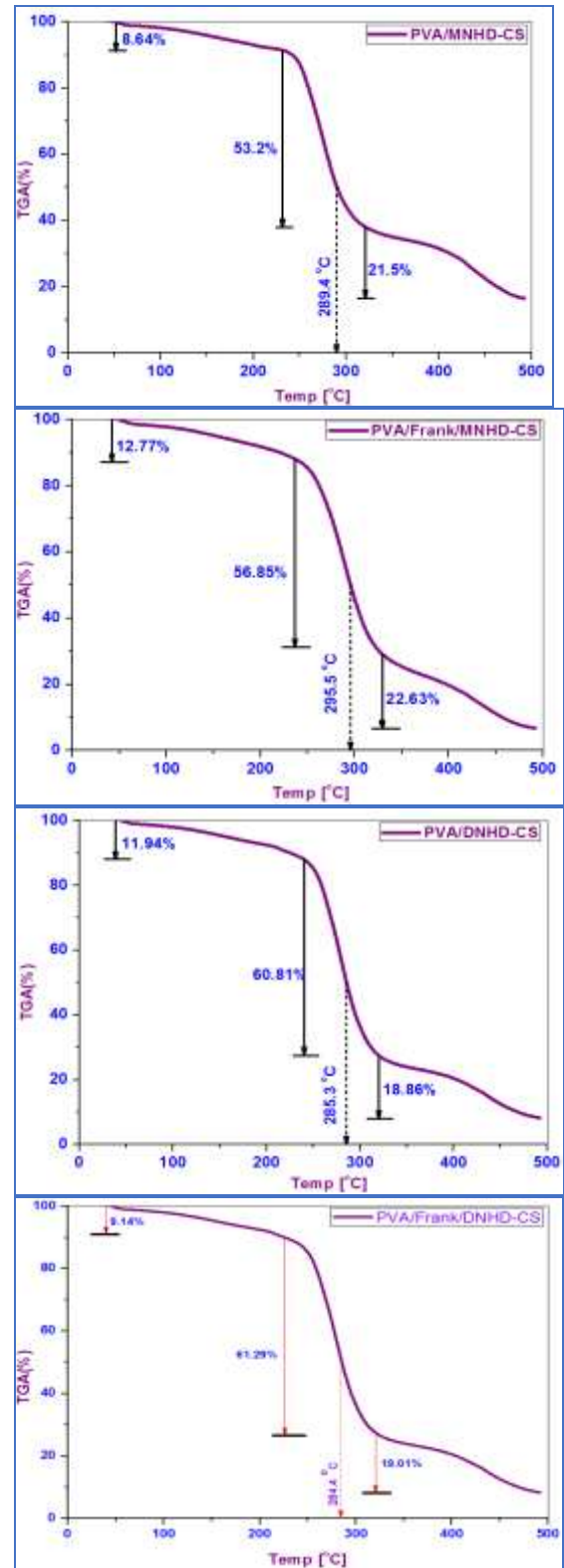
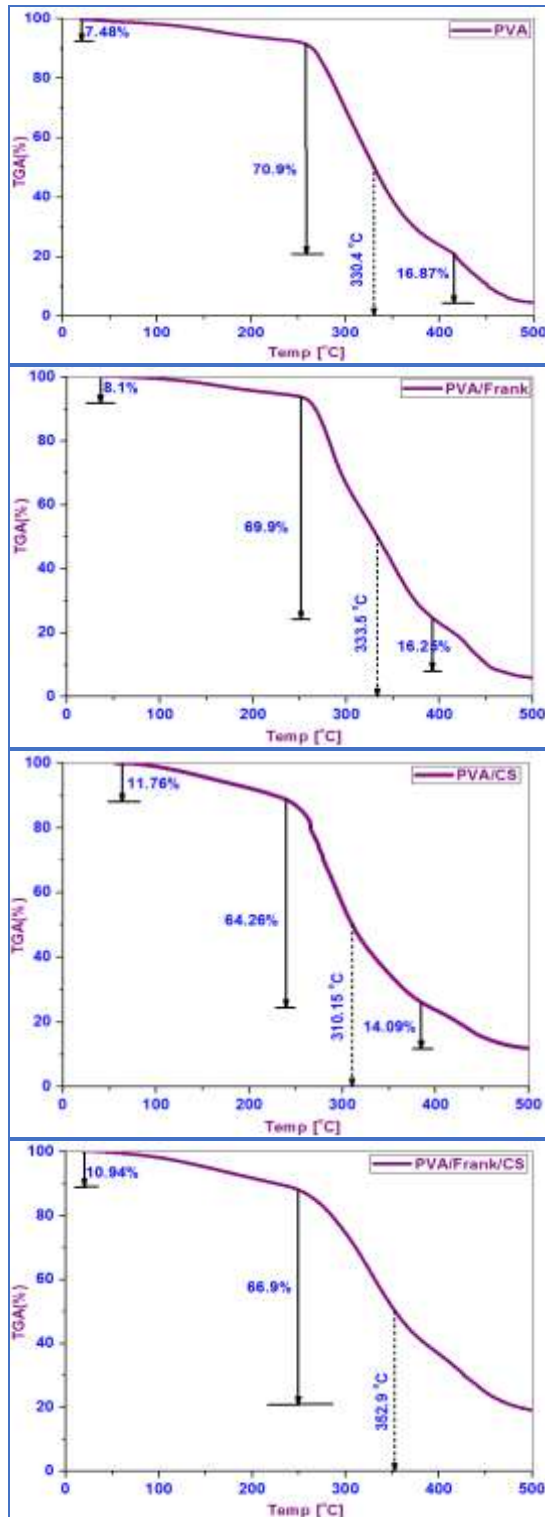


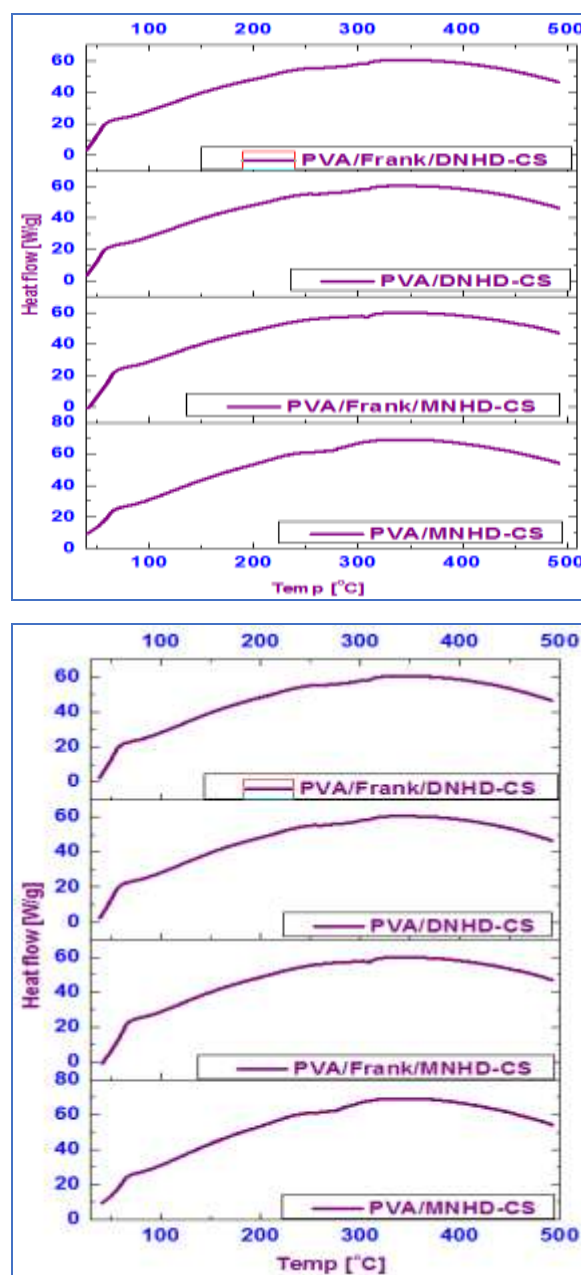
Fig. (3): TGA graphs of different of composite sponge hydrogels

Table (1): Thermal parameter of different formulated sponge hydrogels

Sponge hydrogels	Moisture content (%)	1 st stage	2 nd stage	T ₅₀ (°C)
PVA	7.5	70.9	16.9	330.4
PVA/Frank	8.1	69.9	16.3	333.5
PVA/CS	11.8	64.3	14.1	310.2
PVA/Frank/CS	10.9	66.9	19.6	352.9
PVA/MNHD-CS	8.64	53.2	21.5	289.4
PVA/Frank/MNHD-CS	12.8	56.9	22.6	295.5
PVA/Di-NHD-CS	11.9	60.8	7.9	285.2
PVA/Frank/DNHD-CS	9.1	61.3	19.0	284.4

Figure 4 shows the differential scanning calorimetry (DSC) results for composite PVA hydrogels. Wide endothermic peaks can be seen in the DSC curves in the 70–80 °C temperature range. The release of moisture that was held inside the hydrogel molecules is responsible for these peaks. The findings of this analysis are completely congruent with the authors' earlier work (Mohamed *et al.*, 2018). The relaxation phenomena linked to the hydrogel's crystalline regions is thought to be the cause of the exothermic peaks seen between 105 and 180 °C (Liu *et al.*, 2001). The presence of endothermic peaks in PVA at 217 °C implies the melting of PVA and the subsequent distortion of its crystal structure, which is consistent with the results of a prior study (Gupta *et al.*, 2017). Additionally, the observed decrease in the transition temperature (T_m)

of different PVA composite hydrogels raises the possibility that crystallization is impacted by the crosslinking of PVA with CS derivatives or Frank (Senkevich *et al.*, 2007). The next exothermic peak is caused by the heat-induced breakdown of PVA, which is followed by the loss of water molecules from the polymer's backbone.

**Fig. (4):** DSC analysis of different formulated PVA sponge hydrogels

Gel Fraction

Different hydrogel compositions' effects were evaluated and PVA was found to have an initial gel fraction of $94.84 \pm 4.74\%$. Similarly, the gel fractions of PVA/CS, PVA/MNHD-CS, and PVA/DNHD-CS were reported to be $93.62 \pm 4.68\%$, $86.80 \pm 4.34\%$, and $85.95 \pm 4.30\%$, respectively. The observed phenomena can be linked to polysaccharides' distortion of the PVA crystal structure. The decrease in fractions that follow the replacement of the N-alkyl group with CS raises the possibility that the lipophilic group on the side chain of the CS is a substantial contributor to this outcome. Similar to the results shown in Table 2, the loading of hydrogels improves the aforementioned impact. This shows that PVA experiences considerable cross-linking when Frank oil or CS components are absent (Sung et al., 2010). However, the cross-linking of PVA is reduced when mixed with Frank oil or CS derivatives, leading to an increase in the swelling capabilities of the PVA composite sponges. These features show that the manufactured sponges quickly absorb blood and wound exudate when used. Additionally, a drop in gel % is positively correlated with a decrease in gel strength as well as flexibility. Previous research (Ajjji et al., 2005; Kim et al., 2008) support the conclusions described above.

Swelling behavior

The hydrophilic functional groups of sponges with three-dimensional structures have long been recognized for their capacity to improve the swelling characteristics of the sponges (He et al., 2020). The PVA composite hydrogels' in vitro swelling capabilities were the subject of the experiment, as shown in Table 2 and Figure 5b. When CS was mixed, the swelling ratios showed noticeably decreased water capacity, and this decline was made even worse by N-hexadecanyl CS's increased hydrophobicity. According to these results, the PVA sponge's ability to absorb water was evaluated in the following order: PVA/Frank > PVA/Frank/CS > PVA/CS > PVA > PVA/MNHD-CS > PVA/DNHD-CS. However, when compared to the control combination, the addition of Frank led to a noticeable improvement in water capacity. The study's findings support the proactive use of pre-made sponge hydrogels for the purpose of accelerating wound healing.

In Vitro Degradation

By immersing PVA composite sponge hydrogels in phosphate-buffered saline (PBS) at a temperature of $37\text{ }^{\circ}\text{C}$ for set periods of time, the in vitro degradation of the hydrogels was studied. As shown in Fig. (6), after 72 hours of incubation, the sponge hydrogels that had been treated with Frank and CS

derivatives showed weight losses of up to 35%. When contrasting the two groups, it was shown that the PVA group's body weight decreased by 28.08 1.40%. The findings of this study show that Frank oil has a considerable impact on the rate of degradation seen in sponges. According to this study, the hydrolytic breakdown in vitro may have an effect on the drug release found in this investigation, particularly with regard to Frank oil (Liu *et al.*, 2022; Omer *et al.*, 2021).

Table (2): Porosity of different composite sponge hydrogels

	Porosity (%)
PVA	54.2± 2.7
PVA/Frank	54.2± 2.7
PVA/CS	15.6± 0.8
PVA/Frank/CS	11.6± 0.6
PVA/MNHD-CS	15.9± 0.8
PVA/Frank/MNHD-CS	19.8± 1.0
PVA/DNHD-CS	11.2± 0.6
PVA/Frank/DNHD-CS	14.7± 0.7

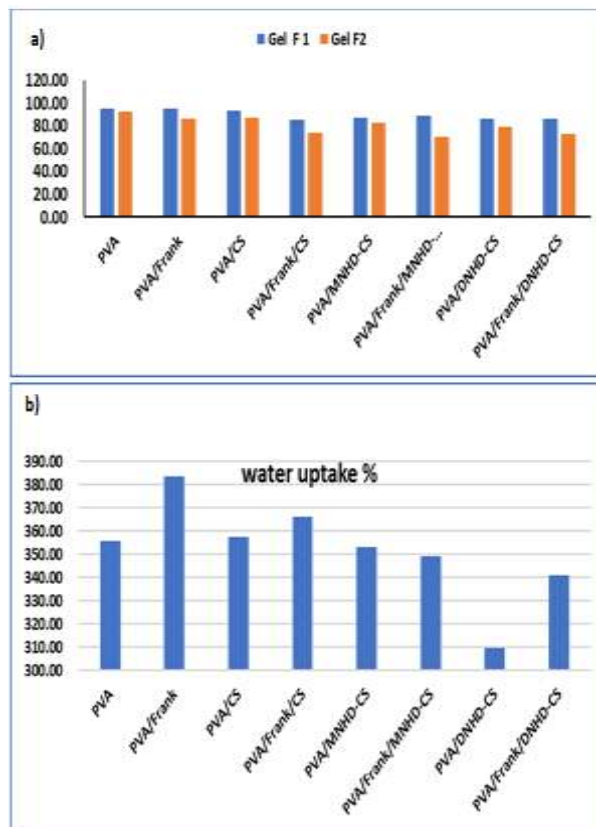


Fig. (5): (a) gel fraction, and (b) water uptakes of different composite sponge hydrogels

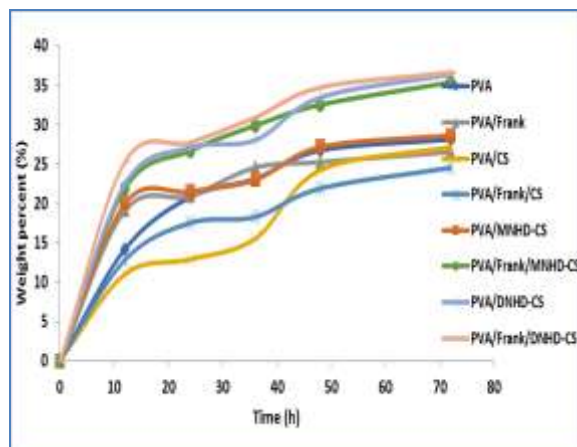


Fig. (6): In vitro hydro-degradation of different composite sponge hydrogels

Antibacterial Activity

Wounds are extremely prone to infection in a catastrophic disaster situation. Thus, it is imperative that the tissue adhesive have high bactericidal

properties. We carried out the zone of inhibition test to assess the sponges' antibacterial properties. Gram-positive bacteria (*B. cereus* and *S. aureus*) and Gram-negative bacteria (*E. coli* and *P. aeruginosa*) formed distinct inhibitory zones with different widths in all of the sponges (Fig. 7). The greatest inhibitory zone was seen against *B. cereus* for all prepared sponges, with *E. coli* and *S. Aureus* coming in second and third. Notably, PVA/Frank/CS showed the highest bacterial inhibition (80 %) across all bacterial strains, followed by PVA/Frank/DNHD-CS (76%), and PVA/Frank/DNHD-CS (70%). When put together, the findings showed that the Frank oil-containing sponges had strong antibacterial action, enabling the use of the substance to stop wound infections. The antibacterial properties of the sponges could perhaps be derived from Frank oil, which has both carboxyl and hydroxyl groups. Frank can adsorb on bacterial cells and interact with the capsular polysaccharide, lipopolysaccharide, and teichoic acid on the bacterial surface, which can cause malfunction or even rupture of the bacterial plasma membrane. Additionally, Frank may enter the cell and meet an alkaline substance, which would cause flocculation and disrupt the physiological processes of the cell (Ma et al., 2017). According to our findings, the sponges worked better against Gram-

positive bacteria than Gram-negative ones (Fig. 7). This could be because the outer lipopolysaccharide layer of *P. aeruginosa* and *E. coli* bacteria's cell walls function as a possible barrier against macromolecules, while the cell walls of Gram-positive bacteria, such as *S. aureus*, are made entirely of peptidoglycan (Qin et al., 2004; Zhao et al., 2015).

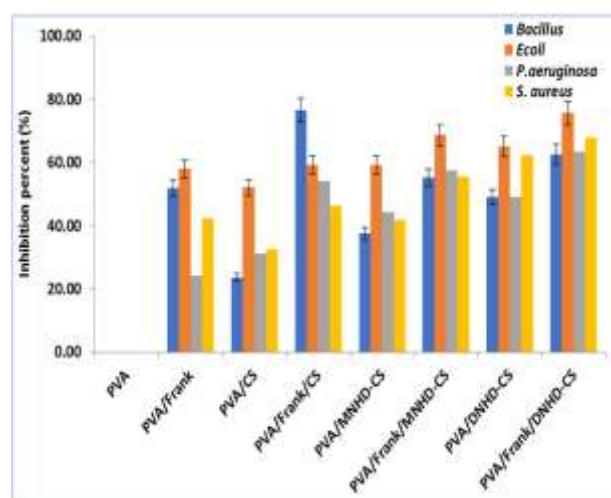


Fig. (7): Antibacterial evaluation of different sponge hydrogels against Gram positive and Gram negative bacterial strains.

Bioactivity investigation

The quantity of phenolic components in essential oils is what gives them their beneficial properties. These molecules provide organisms with vital biological functions, including antioxidant capacities that allow them to neutralise reactive oxygen species (ROS). After being submerged in ethanol, the phenolic content of the sponges under evaluation was measured. The goal of this test was to ascertain how well the formed

sponge hydrogels would release the phenolic-rich Frank oil into the medium. To release the required phenolic combinations, the sponges' structural integrity was used. The PVA sponge used as a negative control in the experiment is shown in (Fig. 8a) to be free of phenolic chemicals. On the other hand, a clear pattern shows that when Frank oil is added to the hydrogel formulation, the phenolic content rises. Figure 8b shows the time evolution of the PVA and other sponge hydrogels' ethanol extracts' ability to decolorize the $ABTS^{++}$ cationic radical. When it came to the $ABTS^{++}$ radical, the PVA hydrogel and other hydrogels without Frank showed a modest level of scavenging effect. The presence of hydroxyl groups in the PVA sponge's backbone is most likely the cause of this action. However, the $ABTS^{++}$ radical scavenging activity was significantly increased when Frank oil was used in sponges. Insofar as they relate to the quantification of total phenolic content, the findings of this study are consistent with the recommendations made in the preceding section. The phenolic chemicals included in Frank oil have the potential to donate electrons, which causes the reduction of $ABTS^{++}$ and subsequent decolorization, which

results in its transformation into a neutral state (Dunnill *et al.*, 2017).

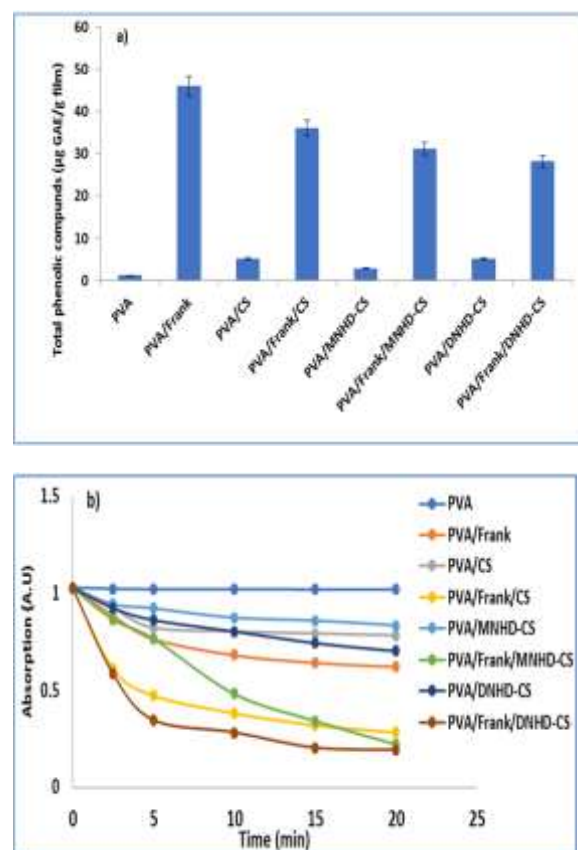


Fig. (8): (a) Total phenolic compounds released from different hydrogels, (b) time-dependent decolorization of $ABTS^{++}$ dye by different hydrogels.

A fundamental quality that is crucial in wound dressings is thought to be blood compatibility (Tamer *et al.*, 2018). This study's goal was to determine whether red blood cells (RBCs) might undergo haemolysis by assessing the hemocompatibility of sponge hydrogels made for this purpose as well as PVA. The haemolytic percentages of the sponges under examination are shown in Figure 9a. In terms of haemolysis, there were no statistically significant differences between PVA supported by

CS derivatives and frankincense oil. But according to the statistical analysis, there were no appreciable differences in PVA between the PVA/Frank hydrogels and other samples. According to the American Society for Testing and Materials' (ASTM) safety criteria, none of the sponge hydrogels produced haemolysis levels greater than 2%. In Fig. (9b), the inquiry into the thrombogenicity of hydrogels was shown. When compared to blood control, PVA sponges have a lower propensity for thrombus development because to their hydrophilic characteristics. On the other hand, thrombus development was significantly increased when CS derivatives and Frank oil were added to PVA hydrogels. This is explained by CS's haemostatic characteristics, which encourage blood clotting.

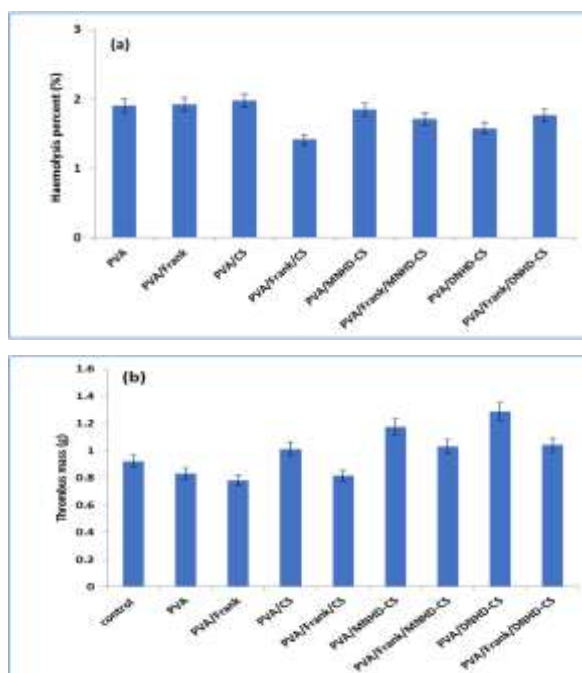


Fig. (9): A) Hemocompatibility, (B) thrombogenicity of different sponge hydrogels

Conclusions

As a conclusion, new sponges based on PVA and enhanced with chitosan and its alkyl derivatives as well as frankincense oil were developed to preclude hemorrhage and bacterial infections. The PVA/Frank-based polymeric hydrogels' physicochemical, antioxidant, and antibacterial properties were evaluated. FT-IR, SEM, swelling ratio, and DSC were used to examine the polymeric interactions, surface morphology, water absorption capacity, thermal stability, thrombogenicity, and hemocompatibility. The existence of molecular interaction between the various components was confirmed by FT-IR. The PVA sponge hydrogel has a distinct porosity structure and a distinctly lamellar appearance, as demonstrated by SEM images. Frank was utilized to improve the porosity of the sponges together with PVA and derivatives of N-hexadecyl CS. Furthermore, DSC provided evidence of the hydrogels' thermal stability. Due to their strong water absorption, they also showed quick bleeding control; the PVA/Frank hydrogel had the highest water uptake efficiency (383.5%). The results also show that Frank oil has a substantial effect on the rate of deterioration; the hydrogel composed of PVA, Frank, and DNHD-CS shows the largest weight loss, up to 35%. The

generated dressing's antibacterial activity was investigated, and the DPPH assay was used to measure the antioxidant activity. The results showed that PVA/Frank/CS had the highest antibacterial activity (80%) against *B. cereus*. The ABTS⁺ radical scavenging activity of sponges containing PVA/Frank hydrogel increased significantly when Frank oil was added, reaching 46% (g GAE/g film). Hemolysis rates of less than 2% were observed in all sponge hydrogels, indicating acceptable blood compatibility and appropriateness for intravenous injection. According to these results, the hydrogels containing Frank may be used as an effective way to create new biomaterials for dressings and as an antibacterial and antioxidant agent for wound care.

Conflicts of interest: There are no conflicts to declare.

References

- Abdelrazik, K.V.T.M.; Aacute, K.; Mohyeldin, M.; Soltes, L. (2016).** Free Radical Scavenger Activity of Cinnamyl Chitosan Schiff Base. *J. Appl. Pharm. Sci.*, 6: 130–136.
- Ajji, Z.; Othman, I.; Rosiak, J.M. (2005).** Production of hydrogel wound dressings using gamma radiation. *Nucl. Instrum. Methods Phys. Res. Sect. B Beam Interact. Mater. At.*, 229: 375–380.
- Alarhayem, A.Q.; Myers, J.G.; Dent, D.; Liao, L.; Muir, M.; Mueller, D.; Nicholson, S.; Cestero, R.; Johnson, M.C.; Stewart, R. (2016).** Time is the enemy: Mortality in trauma patients with hemorrhage from torso injury occurs long before the “golden hour” *Am. J. Surg.* 212, 1101–1105.
- Baylis, J.R.; Yeon, J.H.; Thomson, M.H.; Kazerooni, A.; Wang, X.; St. John, A.E.; Lim, E.B.; Chien, D.; Lee, A.; Zhang, J.Q. (2015).** Self-propelled particles that transport cargo through flowing blood and halt hemorrhage. *Sci. Adv.* 1, e1500379.
- Bakheit S.M, Omer A. (2021).** Antimicrobial activity of *Boswellia papyrifera* essential oil against clinical bacterial pathogens. *Afr. J. Med. Health Sci.* 6: 2.
- Bekana D., Kebede T., Assefa M., Kassa H. (2014).** Comparative Phytochemical Analyses of Resins of *Boswellia* Species (*B. papyrifera* (Del.) Hochst., *B. neglecta* S. Moore, and *B. rivae* Engl.) from Northwestern, Southern, and Southeastern Ethiopia, *Analytical Chemistry*, 2014, 1-9. [dx.doi.org/10.1155/2014/374678](https://doi.org/10.1155/2014/374678).
- Berthet, M.; Gauthier, Y.; Lacroix, C.; Verrier, B.; Monge, C (2017).** Nanoparticle-Based Dressing: The Future of Wound Treatment? *Trends Biotechnol.* 35: 770–784.
- Cao B, Wei XC, Xu XR, Zhang HZ, Luo CH, Feng B, Xu RC, Zhao SY, Du XJ, Han L., Zhang D.K. (2019).** Seeing the Unseen of the Combination of Two Natural Resins, Frankincense and Myrrh: Changes in Chemical Constituents and Pharmacological Activities. *Molecules* 24 (17): 3076–89. [doi: 10.3390/molecules24173076](https://doi.org/10.3390/molecules24173076).
- Chan, L.W.; Wang, X.; Wei, H.; Pozzo, L.D.; White, N.J.; Pun, S.H. (2015).** A synthetic fibrin cross-linking polymer for modulating clot properties and inducing hemostasis. *Sci. Transl. Med.* 7: 277ra229.

- Chen, Y.-N.; Peng, L.; Liu, T.; Wang, Y.; Shi, S.; Wang, H. (2016).** Poly(vinyl alcohol)–Tannic Acid Hydrogels with Excellent Mechanical Properties and Shape Memory Behaviors. *ACS Appl. Mater. Interfaces* 8: 27199–27206.
- Cheng, C.; Peng, X.; Xi, L.; Wan, C.; Shi, S.; Wang, Y.; Yu, X. (2022).** An agar–polyvinyl alcohol hydrogel loaded with tannic acid with efficient hemostatic and antibacterial capacity for wound dressing. *Food Funct.* 13: 9622–9634.
- Dunnill, C.; Patton, T.; Brennan, J.; Barrett, J.; Dryden, M.; Cooke, J.; Leaper, D.; Georgopoulos, N.T. (2017).** Reactive oxygen species (ROS) and wound healing: The functional role of ROS and emerging ROS-modulating technologies for augmentation of the healing process. *Int. Wound J.*, 14: 89–96.
- Fan, X.; Li, Y.; Li, N.; Wan, G.; Ali, M.A.; Tang, K. (2020).** Rapid hemostatic chitosan/cellulose composite sponge by alkali/urea method for massive haemorrhage. *Int. J. Biol. Macromol.* 164: 2769–2778.
- Fang, H.; Wang, J.; Li, L.; Xu, L.; Wu, Y.; Wang, Y.; Fei, X.; Tian, J.; Li, Y. (2019).** A novel high-strength poly(ionic liquid)/PVA hydrogel dressing for antibacterial applications. *Chem. Eng. J.*, 365: 153–164.
- Guan YM, Tao L, Zhu XF, Zang ZZ, Jin C, Chen LH. (2017).** Effects of Frankincense and Myrrh essential oil on transdermal absorption of ferulic acid in Chuanxiong. *Zhongguo Zhong Yao Za Zhi.* 42(17): 3350-3355. doi: 10.19540/j.cnki.cjcmm.20170719.001.
- Guo, B.; Dong, R.; Liang, Y.; Li, M. (2021).** Haemostatic materials for wound healing applications. *Nat. Rev. Chem.* 5: 773–791.
- Guo, S.; Ren, Y.; Chang, R.; He, Y.; Zhang, D.; Guan, F.; Yao, M. (2022).** Injectable Self-Healing Adhesive Chitosan Hydrogel with Antioxidative, Antibacterial, and Hemostatic Activities for Rapid Hemostasis and Skin Wound Healing. *ACS Appl. Mater. Interfaces* 14: 34455–34469.
- Gupta, A. Dhakate, S. R. (2017).** Development of structurally stable electrospun carbon nanofibers from polyvinyl alcohol. *Mater. Res. Express* 4: 45021. <https://doi.org/10.1088/2053-1591/aa6a89>.
- Gurtner, G.C.; Werner, S.; Barrandon, Y.; Longaker, M.T. (2008).** Wound repair and regeneration. *Nature*, 453: 314–321.
- Haidari, H.; Kopecki, Z.; Bright, R.; Cowin, A.J.; Garg, S.; Goswami, N.; Vasilev, K. (2020).** Ultrasmall AgNP-Impregnated Biocompatible Hydrogel with Highly Effective Biofilm Elimination Properties. *ACS Appl. Mater. Interfaces*, 12: 41011–41025.
- Haidari, H.; Bright, R.; Strudwick, X.L.; Garg, S.; Vasilev, K.; Cowin, A.J.; Kopecki, Z. (2021).** Multifunctional ultrasmall AgNP hydrogel accelerates healing of *S. aureus* infected wounds. *Acta Biomater.* 128: 420–434.
- Hamidpour R, Hamidpour S, Hamidpour M, Shahlari M. (2013).** Frankincense: from the selection of traditional applications to the novel phytotherapy for the prevention and treatment of serious diseases. *J. Trad. Compl. Med.*, 3(4): 221–226. doi: 10.4103/2225-4110.119723.
- Han, X.; Rodriguez, D.; Parker, T.L. (2017).** Biological activities of frankincense essential oil in human dermal fibroblasts, *Biochimie Open*, 4: 31–35.
- Hassan, M.A.; Tamer, T.M.; Rageh, A.A.; Abou-Zeid, A.M.; Abd El-Zaher, E.H.F.; Kenawy, E.-R. (2019).** Insight into multidrug-resistant microorganisms from microbial infected diabetic foot

- ulcers. *Diabetes Metab. Syndr. Clin. Res. Rev.* 13: 1261–1270.
- Hassan, N.; Hendy, A.; Ebrahim, A.; Tamer, T.M. (2021).** Synthesis and evaluation of novel O-functionalized aminated chitosan derivatives as antibacterial, antioxidant and anticorrosion for 316L stainless steel in simulated body fluid. *J. Saudi Chem. Soc.*, 25: 101368.
- Hassan, M.A.; Abd El-Aziz, S.; Elbadry, H.M.; El-Aassar, S.A.; Tamer, T.M. (2021).** Prevalence, antimicrobial resistance profile, and characterization of multi-drug resistant bacteria from various infected wounds in North Egypt. *Saudi J. Biol. Sci.* 29: 2978–2988.
- He, J.; Shi, M.; Liang, Y.; Guo, B. (2020).** Conductive adhesive self-healing nanocomposite hydrogel wound dressing for photothermal therapy of infected full-thickness skin wounds. *Chem. Eng., J.* 394: 124888.
- He, Y.; Liu, K.; Zhang, C.; Guo, S.; Chang, R.; Guan, F.; Yao, M. (2022).** Facile preparation of PVA hydrogels with adhesive, self-healing, antimicrobial, and on-demand removable capabilities for rapid hemostasis. *Biomater. Sci.*, 10: 5620–5633.
- Kenawy, E.R.; Abdel-Hay, F.I.; Tamer, T.M.; Ibrahim, E.M.A.-E.; Eldin, M.S.M. (2019).** Antimicrobial activity of novel modified aminated chitosan with aromatic esters. *Polym. Bull.* 77: 1631–1647.
- Khalifa S. A.M., Kotb S. M., El-Seedi S. H., Nahar L., Sarker S. D., Guo Z., Zou X., Musharraf S. G., Jassbi A. R., Du M., El-Seedi H. R. (2023).** Frankincense of *Boswellia sacra*: Traditional and modern applied uses, pharmacological activities, and clinical trials. *Industrial Crops and Products.* 203: 117106.
- Kim, J.O.; Choi, J.Y.; Park, J.K.; Kim, J.H.; Jin, S.G.; Chang, S.W.; Li, D.X.; Hwang, M.R.; Woo, J.S.; Kim, J.A. (2008).** Development of clindamycin-loaded wound dressing with polyvinyl alcohol and sodium alginate. *Biol. Pharm. Bull.* 31: 2277–2282.
- Kim, K.; Ryu, J.H.; Koh, M.Y.; Yun, S.P.; Kim, S.; Park, J.P.; Jung, C.W.; Lee, M.S.; Seo, H.I.; Kim, J.H. (2021).** Coagulopathy-independent, bioinspired hemostatic materials: A full research story from preclinical models to a human clinical trial. *Sci. Adv.*, 7: eabc9992.
- King, D.R. (2019).** Initial Care of the Severely Injured Patient. *N. Engl. J. Med.*, 380: 763–770.
- Lestari, W.; Yusry, W.N.A.W.; Haris, M.S.; Jaswir, I.; Idrus, E. (2020).** A glimpse on the function of chitosan as a dental hemostatic agent. *Jpn. Dent. Sci. Rev.* 56: 147–154.
- Le-Vinh, B.; Le, N.-M.N.; Nazir, I.; Matuszczak, B.; Bernkop-Schnürch, A. (2019).** Chitosan based micelle with zeta potential changing property for effective mucosal drug delivery. *Int. J. Biol. Macromol.*, 133: 647–655.
- Li, Y., Qing, S., Zhou, J., Yang, G. (2014).** Evaluation of bacterial cellulose/hyaluronan nanocomposite biomaterials. *Carbohydr. Polym.* 103: 496–501. doi.org/10.1016/j.carbpol.2013.12.059.
- Li, J.; Wu, Y.; Zhao, L. (2016).** Antibacterial activity and mechanism of chitosan with ultra-high molecular weight. *Carbohydr. Polym.*, 148: 200–205.
- Liu, T. Petermann, J. (2001).** Multiple melting behavior in isothermally cold-crystallized isotactic polystyrene. *Polymer* 42: 6453–6461. doi.org/10.1016/S0032-3861(01)00173-2

- Liu, X., You, L., Tarafder, S., Zou, L., Fang, Z., Chen, J., Lee, C. H., Zhang, Q. (2019).** Curcumin-releasing chitosan/alginate membrane for skin regeneration. *Chem. Eng. J.* 359: 1111–1119. doi.org/10.1016/j.cej.2018.11.073 (2019).
- Ma, Y.; Yao, J.; Liu, Q.; Han, T.; Zhao, J.; Ma, X.; Tong, Y.; Jin, G.; Qu, K.; Li, B. (2020).** Liquid Bandage Harvests Robust Adhesive, Hemostatic, and Antibacterial Performances as a First-Aid Tissue Adhesive. *Adv. Funct. Mater.*, 30: 2001820-2001833. <https://doi.org/10.1002/adfm.202001820>
- Ma, Z., Garrido-Maestu, A. Jeong K.C. (2017).** Application, mode of action, and in vivo activity of chitosan and its micro- and nanoparticles as antimicrobial agents: A review. *Carbohydr. Polym.* 176: 257-265.
- Mohammed, G., El Sayed, A. M.; Morsi, W. M. (2018).** Spectroscopic, thermal, and electrical properties of MgO/polyvinyl pyrrolidone/ polyvinyl alcohol nanocomposites. *J. Phys. Chem. Solids*, 115: 238–247. <https://doi.org/10.1016/j.jpcs.2017.12.050>.
- Mansur, H.S.; Sadahira, C.M.; Souza, A.N.; Mansur, A.A.P. (2008).** FTIR spectroscopy characterization of poly(vinyl alcohol) hydrogel with different hydrolysis degree and chemically crosslinked with glutaraldehyde. *Mater. Sci. Eng. C*, 28: 539–548.
- Mansour, H.; El-Sigeny, S.; Shoman, S.; Abu-Serie, M.M.; Tamer, T.M. (2022).** Preparation, Characterization, and Bio Evaluation of Fatty N- Hexadecanyl Chitosan Derivatives for Biomedical Applications. *Polymers*, 14: 4011. <https://doi.org/10.3390/polym14194011>
- Mansur, H.S.; Oréface, R.L.; Mansur, A.A.P. (2004).** Characterization of poly(vinyl alcohol)/poly(ethylene glycol) hydrogels and PVA-derived hybrids by small-angle X-ray scattering and FTIR spectroscopy. *Polymer*, 45: 7193–7202.
- Mohy Eldin, M.S.; Omer, A.M.; Wassel, M.A.; Tamer, T.M.; Abd Elmonem, M.S.; Ibrahim, S.A. (2015).** Novel smart pH-sensitive chitosan grafted alginate hydrogel microcapsules for oral protein delivery: I. preparation and characterization. *Int. J. Pharm. Pharm. Sci.*, 7: 320–326.
- Omer, A.M.; Ammar, Y.; Mohamed, G.; ElBaky, Y.A.; Tamer, T.M. (2019).** Preparation of Isatin/chitosan schiff base as novel antibacterial biomaterials. *Egypt. J. Chem.* 62: 123–131.
- Omer, A.M.; Ziora, Z.M.; Tamer, T.M.; Khalifa, R.E.; Hassan, M.A.; Mohy-Eldin, M.S.; Blaskovich, M.A.T. (2021).** Formulation of Quaternized Aminated Chitosan Nanoparticles for Efficient Encapsulation and Slow Release of Curcumin. *Molecules*. 26: 449.
- Peng, X.; Xia, X.; Xu, X.; Yang, X.; Yang, B.; Zhao, P.; Yuan, W.; Chiu, P.W.Y.; Bian, L. (2021).** Ultrafast self-gelling powder mediates robust wet adhesion to promote healing of gastrointestinal perforations. *Sci. Adv.*, 7: eabe8739.
- Pereira, R.F.; Bártolo, P.J. (2008).** Traditional Therapies for Skin Wound Healing. *Adv. Wound Care* 2016, 5: 208–229.
- Qi, X.; Hu, X.; Wei, W.; Yu, H.; Li, J.; Zhang, J.; Dong, W. (2015).** Investigation of Salecan/poly(vinyl alcohol) hydrogels prepared by freeze/thaw method. *Carbohydr. Polym.* 118: 60–69.
- Qin C, Xiao Q, Li H, Fang M, Liu Y, Chen X, Li Q. (2004).** Calorimetric studies of the action of chitosan-N-2-hydroxypropyl trimethyl ammonium chloride on the growth of microorganisms. *Int. J. Biol. Macromol.* 34(1-2): 121-6.

- Raafat, D.; Sahl, H.-G. (2009).** Chitosan and its antimicrobial potential—A critical literature survey. *Microb. Biotechnol.*, 2: 186–201.
- Ren, J.; Yin, X.; Chen, Y.; Chen, Y.; Su, H.; Wang, K.; Zhang, L.; Zhu, J.; Zhang, C. (2020).** Alginate hydrogel-coated syringe needles for rapid haemostasis of vessel and viscera puncture. *Biomaterials* 249: 120019.
- Saied, M.A., Kamel, N.A., Ward, A.A. (2020).** Novel Alginate Frankincense Oil Blend Films for Biomedical Applications. *Proc. Natl. Acad. Sci., India, Sect. B. Biol. Sci.*, 90: 303–312. <https://doi.org/10.1007/s40011-019-01103-y>.
- Senkevich, S. I., Druzhinina, T. V., Kharchenko, I. M., Kryazhev, Y. G. (2007).** Thermal transformations of polyvinyl alcohol as a source for the preparation of carbon materials. *Solid Fuel Chem.* 41: 45–51. doi.org/10.3103/S0361521907010107.
- Shaban, N. Z., Yehia, S. A., Shoueir, K. R., Saleh, S. R., Awad, D., & Shaban, S. Y. (2019).** Design, DNA binding and kinetic studies, antibacterial and cytotoxic activities of stable dithiophenolato titanium(IV)-chitosan Nanocomposite. *Journal of Molecular Liquids*, 287: 111002. <https://doi.org/10.1016/j.molliq.2019.111002>.
- Sharma A., Chhikara S., Ghodekar S. N., Bhatia S., Kharya M. D., Gajbhiye V., Mann A. S., Namdeo A.G., Mahadik K. R. (2009).** Phytochemical and Pharmacological Investigations on *Boswellia serrata*, *Phcog Rev.* 3(5): 206–215.
- Shefa, A.A.; Amirian, J.; Kang, H.J.; Bae, S.H.; Jung, H.-I.; Choi, H.-j.; Lee, S.Y.; Lee, B.-T. (2017).** In vitro and in vivo evaluation of effectiveness of a novel TEMPO-oxidized cellulose nanofiber-silk fibroin scaffold in wound healing. *Carbohydr. Polym.* 177: 284–296.
- Sultana, T.; Hossain, M.; Rahaman, S.; Kim, Y.S.; Gwon, J.-G.; Lee, B.-T. (2021).** Multi-functional nanocellulose-chitosan dressing loaded with antibacterial lawsone for rapid hemostasis and cutaneous wound healing. *Carbohydr. Polym.*, 272: 118482.
- Sung, J.H.; Hwang, M.R.; Kim, J.O.; Lee, J.H.; Kim, Y.I.; Kim, J.H.; Chang, S.W.; Jin, S.G.; Kim, J.A.; Lyoo, W.S. (2010).** Gel characterisation and in vivo evaluation of minocycline-loaded wound dressing with enhanced wound healing using polyvinyl alcohol and chitosan. *Int. J. Pharm.* 392: 232–240.
- Tamer, T.M.; Valachová, K.; Hassan, M.A.; Omer, A.M.; El-Shafeey, M.; Mohy Eldin, M.S.; Šoltés, L. (2018).** Chitosan/hyaluronan/edaravone membranes for anti-inflammatory wound dressing: In vitro and in vivo evaluation studies. *Mater. Sci. Eng. C*, 90: 227–235.
- Tamer, T.M.; Collins, M.N.; Valachová, K.; Hassan, M.A.; Omer, A.M.; Mohy-Eldin, M.S.; Švík, K.; Jurčík, R.; Ondruška, E.; Biró, C. (2018).** Loaded Chitosan-Hyaluronan Composite Membranes for Wound Healing. *Materials* 11, 569–581.
- Tamer, T.M., Alsehli, M.H., Omer, A.M., Mohy-Eldin, M.S., Hassan, M.A. (2021).** Development of polyvinyl alcohol/ kaolin sponges stimulated by marjoram as hemostatic, antibacterial, and antioxidant dressings for wound healing promotion. *International Journal of Molecular Sciences* 22(23): 13050.
- Tamer, T.M.; Sabet, M.M.; Omer, A.M.; Abbas, E.; Eid, A.I.; Mohy-Eldin, M.S.; Hassan, M.A. (2021).** Hemostatic and antibacterial PVA/Kaolin composite sponges loaded with penicillin–

- streptomycin for wound dressing applications. *Sci. Rep.* 11: 3428.
- Tamer, T.M., Sabet, M.M., Alhalili, Z.A.H., Mohy-Eldin, M.S., Hassan, M.A. (2022).** Influence of Cedar Essential Oil on Physical and Biological Properties of Hemostatic, Antibacterial, and Antioxidant Polyvinyl Alcohol/Cedar Oil/Kaolin Composite Hydrogels. *Pharmaceutics*, 14(12): 2649.
- Tamer, T.M.; Hassan, M.A.; Valachová, K.; Omer, A.M.; El-Shafeey, M.E.; Eldin, M.S.M.; Šoltés, L. (2020).** Enhancement of wound healing by chitosan/hyaluronan polyelectrolyte membrane loaded with glutathione: In vitro and in vivo evaluations. *J. Biotechnol.* 310: 103–113.
- Tian, B.; Liu, Y.; Liu, J. (2021).** Chitosan-based nanoscale and non-nanoscale delivery systems for anticancer drugs: A review. *Eur. Polym. J.*, 154: 110533.
- Wang, H.; Zhu, H.; Fu, W.; Zhang, Y.; Xu, B.; Gao, F.; Cao, Z.; Liu, W. (2017).** A High Strength Self-Healable Antibacterial and Anti-Inflammatory Supramolecular Polymer Hydrogel. *Macromol. Rapid Commun.*, 38: 1600695.
- Wang, K.; Wang, J.; Li, L.; Xu, L.; Feng, N.; Wang, Y.; Fei, X.; Tian, J.; Li, Y. (2019).** Synthesis of a novel anti-freezing, non-drying antibacterial hydrogel dressing by one-pot method. *Chem. Eng. J.*, 372: 216–225.
- Xie, M.; Zeng, Y.; Wu, H.; Wang, S.; Zhao, J. (2022).** Multifunctional carboxymethyl chitosan/oxidized dextran/sodium alginate hydrogels as dressing for hemostasis and closure of infected wounds. *Int. J. Biol. Macromol.* 219: 1337–1350.
- Yin, L.; Fei, L.; Tang, C.; Yin, C. (2007).** Synthesis, characterization, mechanical properties and biocompatibility of interpenetrating polymer network–superporous hydrogel containing sodium alginate *Polym. Int.*, 56 (12): 1563-1571.
- Yagi S, Babiker R, Tzanova T, Schohn H. (2016).** Chemical composition, antiproliferative, antioxidant and antibacterial activities of essential oils from aromatic plants growing in Sudan. *Asian Pac. J. Trop Med.*, 9(8): 763-70. doi: 10.1016/j.apjtm.2016.06.009.
- Yuan, Y.; Tan, W.; Mi, Y.; Wang, L.; Qi, Z.; Guo, Z. (2024).** Effect of Hydrophobic Chain Length in Amphiphilic Chitosan Conjugates on Intracellular Drug Delivery and Smart Drug Release of Redox-Responsive Micelle. *Mar. Drugs*, 22: 18-36. <https://doi.org/10.3390/md22010018>.
- Zhao X, Li P, Guo B, Ma PX. (2015).** Antibacterial and conductive injectable hydrogels based on quaternized chitosan-graft-polyaniline/oxidized dextran for tissue engineering. *Acta Biomater.* 26: 36-48. doi: 10.1016/j.actbio.2015.08.006.
- Zhao, X.; Guo, B.; Wu, H.; Liang, Y.; Ma, P.X. (2018).** Injectable antibacterial conductive nanocomposite cryogels with rapid shape recovery for noncompressible hemorrhage and wound healing. *Nat. Commun.*, 9: 2784-2801.
- Zhao, X.; Liang, Y.; Huang, Y.; He, J.; Han, Y.; Guo, B. (2020).** Physical Double-Network Hydrogel Adhesives with Rapid Shape Adaptability, Fast Self-Healing, Antioxidant and NIR/pH Stimulus-Responsiveness for Multidrug-Resistant Bacterial Infection and Removable Wound Dressing. *Adv. Funct. Mater.*, 30: 1910748.
- Zhou, T.; Chen, S.; Ding, X.; Hu, Z.; Cen, L.; Zhang, X. (2021).** Fabrication and Characterization of Collagen/PVA Dual-Layer Membranes for Periodontal Bone Regeneration. *Front. Bioeng. Biotechnol.*, 9: 630977.

Zhou, Z.; Xiao, J.; Guan, S.; Geng, Z.; Zhao, R.; Gao, B. (2022). A hydrogen-bonded antibacterial curdlan-tannic acid hydrogel with an antioxidant and hemostatic function for wound healing. *Carbohydr. Polym.*, 285: 119235.

Zhu XF, Luo J, Guan YM, Yu YT, Jin C, Zhu WF, Liu HN. (2017). [Effects of Frankincense and Myrrh essential oil on

transdermal absorption in vitro of Chuanxiong and penetration mechanism of skin blood flow]. *Zhongguo Zhong Yao Za Zhi.*, 42(4): 680-685. doi: 10.19540/j.cnki.cjmm.20170103.025.

تصنيع وخصائص وثباتية زيت اللبان المحمل علي الكيتوزان الدهني/البولي فينيل الهلاميات المائية لشفاء الجروح

تامر تامر^١، سامية السجيني^٢، ساره شومان^٢، هناء منصور^{٢*}

^١ مدينة الأبحاث العلمية و التطبيقات التكنولوجية بالاسكندرية
^٢ كلية العلوم جامعة كفر الشيخ

باعتبارها هيدروجيل، فإن ضمادات الجروح المصنوعة من البولييمرات وزيت اللبان (فرانك) يمكن أن تعمل بشكل جيد للغاية. الهدف من الدراسة الحالية هو تحضير الهلاميات المائية الإسفنجية فرانك مع مشتقات الكيتوزان N-hexadecanyl الدهنية في كحول البولي فينيل (PVA) كعامل مضاد للجراثيم. تم تقييم النشاط الحيوي والأداء الفيزيوكيميائي للهيدروجيلات البوليمرية المعتمدة على PVA/Frank. تمت دراسة التفاعلات البوليمرية، والتشكل السطحي، والقدرة على امتصاص الماء، والنبات الحراري، والتخثر والتوافق الدموي بواسطة FT-IR، و SEM، ونسبة التورم وتظهر صور SEM أن هيدروجيل إسفنجية PVA لها بنية مسامية مميزة وتظهر طبقة صفائحية بشكل ملحوظ، وتظهر كالوريمتر المسح الضوئي التفاضلي (DSC) الثبات الحراري للهيدروجيلات. علاوة على ذلك، فقد أظهروا تحكماً سريعاً في النزيف بسبب امتصاصهم العالي للماء، حيث يتمتع هيدروجيل PVA/Frank بأعلى كفاءة في امتصاص الماء (٣٨٣.٥%). توضح النتائج أيضاً أن زيت فرانك يؤثر بشكل كبير على معدل التحلل، حيث أظهر هيدروجيل PVA/Frank/DNHD-CS أكبر خسارة في الوزن تصل إلى ٣٥%. تم فحص النشاط المضاد للبكتيريا، وتم اختبار مضادات الأكسدة باستخدام مقياس DPPH وفقاً للنتائج، كان لـ PVA/Frank/CS أقوى نشاط مضاد للجراثيم ضد *B. cereus* (80%). أدى استخدام زيت فرانك في الإسفنج مع PVA/Frank هيدروجيل إلى زيادة كبيرة في نشاط ABTS⁺⁺ الكسح الجذري، حيث وصل إلى ٤٦% (جرام/GAE جرام فيلم). كان لدى جميع الهلاميات المائية الإسفنجية معدلات انحلال الدم أقل من ٢٪، مما يشير إلى توافق الدم الجيد وملاءمته للحقن في الوريد. تشير هذه النتائج إلى أن الهلاميات المائية التي تحتوي على فرانك لها استخدام محتمل كعامل مضاد للبكتيريا ومضاد للأكسدة للعناية بالجروح، وكذلك لتطوير مواد حيوية جديدة للضمادات.